IOP Conf. Series: Materials Science and Engineering **161** (2016) 012045 doi:10.1088/1757-899X/161/1/012045

Random lattice structures. Modelling, manufacture and FEA of their mechanical response

G Maliaris[1], I T Sarafis[2], T Lazaridis[2], A Varoutoglou[2] and G Tsakataras[2]

[1]Laboratory for Special Engineering, Department of Electrical & Computer Engineering, School of Engineering, Democritus University of Thrace, GR67100, Xanthi, Greece

Email: gmaliari@ee.duth.gr

[2]Mechanical Engineering Department, Technological Educational Institute of East Macedonia-Thrace, Agios Loukas, GR65404, Kavala, Greece

Abstract. The implementation of lightweight structures in various applications, especially in Aerospace/ Automotive industries and Orthopaedics, has become a necessity due to their exceptional mechanical properties with respect to reduced weight. In this work we present a Voronoi tessellation based algorithm, which has been developed for modelling stochastic lattice structures. With the proposed algorithm, is possible to generate CAD geometry with controllable structural parameters, such as porosity, cell number and strut thickness. The digital structures were transformed into physical objects through the combination of 3D printing technics and investment casting. This process was applied to check the mechanical behaviour of generated digital models. Until now, the only way to materialize such structures into physical objects, was feasible through 3D printing methods such as Selective Laser Sintering/ Melting (SLS/ SLM). Investment casting possesses numerous advantages against SLS or SLA, with the major one being the material variety. On the other hand, several trials are required in order to calibrate the process parameters to have successful castings, which is the major drawback of investment casting. The manufactured specimens were subjected to compression tests, where their mechanical response was registered in the form of compressive load – displacement curves. Also, a finite element model was developed, using the specimens' CAD data and compression test parameters. The FE assisted calculation of specimen plastic deformation is identical with the one of the physical object, which validates the conclusions drawn from the simulation results. As it was observed, strut contact is initiated when specimen deformation is approximately 5mm. Although FE calculated compressive force follows the same trend for the first 3mm of compression, then diverges because of the elasto-plastic FE model type definition and the occurred remeshing steps.

1. Introduction

Biomimicry, man effort to imitate nature strategies in solving human problems has found many applications during man evolution. In this respect, humans managed to imitate the foam-like structures, widely used by nature, by manufacturing metal foams and honeycomb structures using various production methods [1]. Nowadays, metal foams are used for a broad range of applications in aerospace/ automotive industries and recently in orthopaedics. They combine unique properties such as high strength to weight ratios as well as energy absorption characteristics [2]. In the previous mentioned examples two different cellular arrangements are introduced; ordered and stochastic one. The geometry of random lattices (metal foams) consists of irregular, non-periodic cells which form a

network of interconnecting walls or struts. On the other hand, regular lattice structures (honeycomb) are formed by the repetitive placement, at the same distance in 3D space, of a representative cell.

Understanding mechanical behaviour is the key parameter for the proper adoption of cellular materials to various applications. Experimental testing combined with finite element analysis has proved to be a solid method for material characterization. In the case of cellular geometries with stochastic arrangement, experimental testing is an easy task in contrast to FEA where geometry definition, an essential step towards seamlessly FE model setup, imposes difficulties due to random structure nature. Various solutions have been proposed by researchers in order to simplify the effort required for the representation of cellular geometry. The most accurate method depends on the reconstruction of the real foam geometry using micro CT scans. Although μCT has gained popularity nowadays, it involves the operation of expensive infrastructure which normally generates huge amount of data that require a time consuming process to translate raw data into geometry. On the other hand, methods that rely on mathematical approximations of the lattice geometry using statistical analysis of pivotal geometric data represent the majority of the published work on this scientific field. Initial efforts for foam modelling relied on previously submitted articles on foam froth geometry approximation. In these investigations the Kelvin cell was used which partitions space with minimum surface area for identical cells [3, 4]. Although it is proven that Kelvin tetrakaidecahedron cannot accurately represent foam geometry, because the natural variations of cell size and shape are not considered [5], researchers kept on using it upon recently [6], mainly as a reference structure. A promising method, recently employed by many researchers, is the generation of irregular cells applying the Voronoi tessellation technique. This technic is used to partition 3D space into random polyhedra. The geometric features of the generated polyhedra are later used in lattice structure modelling.

The mechanical behaviour of cellular solids has been thoroughly investigated by various researchers the last 15 years. The elastic response of open cell foams was studied by [6, 7, 8]. In their investigations researchers considered the effect of various parameters such as relative density, cell irregularity, cell shape and strut cross sectional variations. It was found that relative density and cell irregularity are the dominant parameters affecting the elastic moduli. Also, as energy absorbers, foams are frequently subjected to dynamic loadings or impacts. Therefore, it is quite significant to analyse the large plastic deformation behaviour considering also dynamic phenomena such as rate dependent material properties. Large plastic deformation regime of cellular materials consists of two regions; extended stress plateau and densification region [2]. In order to capture the densification effect through FE analysis, self-contact between struts should be implemented in the developed FE models. The later requirement increases the computation effort by a large margin, so simplification of the strut FE modelling is a necessary step towards efficient computational time management. Two dimensional FE models [9, 10] and beam-based strut realization [6, 10, 11] are the main methods which are commonly applied.

The geometrical characterization of stochastic cellular structures is achieved through the determination of geometric parameters such as cell irregularity, strut cross sectional shape, strut equivalent radius, porosity. Up to recently it was not possible to prescribe these parameters, since they are coupled to the applied processing method, thus they follow physical laws and remain uncontrolled parameters. The last years, the emergence of various additive manufacturing methods, with enhanced accuracy, rendered feasible the materialization of stochastic and ordered lattice structures. The mechanical behaviour of 3D – printed ordinate structures using the DMLS (Direct Metal Laser Sintering) or SLM (Selective Laser Melting) additive technologies where investigated by several researchers [12 – 14]. Relationship between unit cell type and porosity and the fatigue behaviour of selective laser melted meta-biomaterials was studied by Amin Yavari et al. The failure mechanisms of additively manufactured porous biomaterials considering porosity and unit cell type was investigated in [13]. The effects of build orientation and heat treatment on the microstructure and mechanical properties of selective laser melted Ti6Al4V lattice structures was explored in [14]. The above mentioned research papers were focused on metallic lattice structures which were modelled using specific unit cells.

In the present study the random lattice structures were created applying the voronoi tessellation technic. The Voronoi tessellation (or Voronoi diagram) is a space partitioning method which creates polyhedral (cells), when applied in 3D space. The struts are modelled as solid cylinders with constant radius. With the proposed algorithm is possible to control various geometric characteristics such as porosity and cell mean volume. The modelled geometry is then 3D printed with a photosensitive castable resin. The final parts are manufactured by investment casting. The specific manufacturing method permits the use of various materials such as steel alloys, aluminium alloys, titanium alloys, gold, silver, platinum, etc.. The casted parts are subjected to compressive experiments which are coupled to FEA simulations in order to investigate their mechanical behaviour. The use of a self-contact algorithm is considered in the FEA models so that the interaction between the struts can be detected, which is crucial for capturing material behaviour in the densification area.

2. Solid modelling

The Voronoi tessellation (or Voronoi diagram) is a space partitioning method which creates polyhedra, when applied to a 3D geometry (a control volume) that share a common characteristic. The distance between the seed point of a polyhedron and any point included in the specific polyhedron is the minimum one with respect to other seed points. The tessellation is applied to N randomly distributed seed points into a control volume, which is usually a simple geometry such as cube, cylinder, sphere, etc.. The employed seed point distribution method is of a great interest since it defines the statistical distribution of pivotal geometric characteristics. In the next step, the neighbouring points are connected with lines which are then bisected by their perpendicular planes. For a given seed point, its Voronoi cell is defined by the smallest polyhedron that contains that point. The above mentioned procedure is presented in figure 1 for 10 seed points.

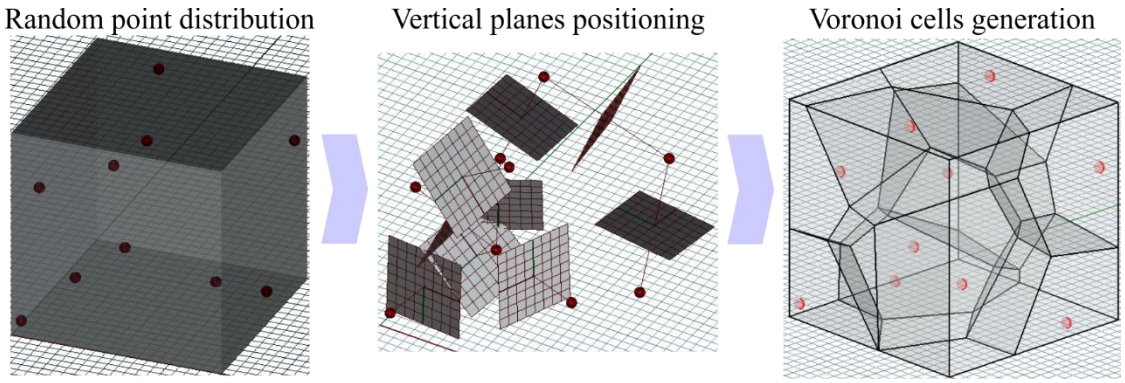

Figure 1: The Voronoi tessellation procedure

The edges of the Voronoi cells form the skeleton which can be appropriately dressed to represent the struts of the lattice structure. The majority of the researchers use the vertices of the cells in order to define beam elements during the FE model definition [4, 6, 10, 15, 16, 17]. Although this simplification leads to geometries that do not capture the cross section variation along strut length and mass concentration at the junctions, is a preferred method of strut modelling in order to limit the required computational effort.

In this work the extracted Voronoi cell edges are “dressed” with solid cylinders with constant radius, to appropriately capture strut deformation during compression, after contact has been established. This approximation is more realistic than the definition of beam elements and provides more insight for the determination of the structure failure mode. After the properly positioning of the cylinders in 3D space, another algorithm is applied that joins the cylinders together. During that procedure, some geometrical errors occur which are overcome by applying a wrap function on the whole geometry. The latter function applies a wrapping surface on the selected entities and can easily fix topology errors such as small tunnels, intersecting triangles, entrapped surfaces, etc. The result is a watertight mesh with clean geometry. A sample lattice structure created with the above mentioned methodology is presented in figure 2.

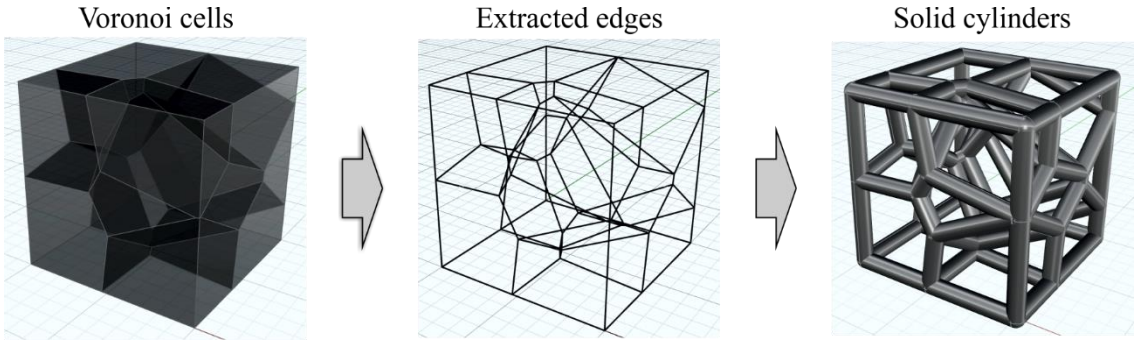

Figure 2: Solid modelling procedure

3. Lattice structure manufacturing

The developed solid modelling algorithm was used to create lattice structures with various characteristics such as porosity and strut radius. The manufacturing route of the digital lattices starts with the 3D printing of the geometry with a photosensitive castable resin. The specific type of photosensitive resins have gained great attention, especially from goldsmiths, which is attributed to the fact that have provided a mean for producing intricate jewellery designs using a well-established production method such as investment casting. The modelled stochastic lattices were printed using two different 3D printers, a consumer level printer (Formlabs Form1+) and a professional one (Asiga FreeForm Pro75). Both utilize the SLA technic (Stereolithography) but use different light sources. The Form1+ a UV laser, where Asiga a high definition UV DLP projector. The printed samples were transformed to metal lattices by investment casting using the Orotig Speedcast 220MJ – Ti casting machine. The specific machine has automated casting cycles, where the metal is melted by the electric arc in presence of Argon-gas. When the casting takes place, the molten metal is pushed down into the flask by a controlled Argon-gas overpressure. This make possible to obtain very compact, oxidation-free casting extremely accurate in details and quite precise and fitting even in very diminutive sections, thus is the perfect candidate for manufacturing the stochastic lattices.

The initial trials revealed certain constrains of the casting procedure which relate with the geometric characteristics of the modelled structures. The cell size and the strut radius should be large enough to allow continuous metal flow and also removal of the investment material with little effort. As it is observed in figure 3, the casting was unsuccessful as both geometric constrains did not have appropriate values.

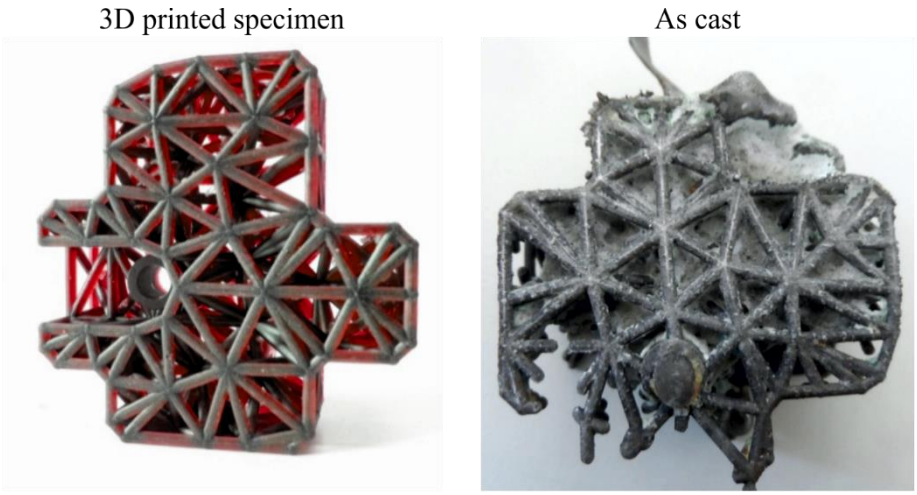

Resin: Asiga SuperCAST, Printing layer height: 10μm
Casting material: Steel 304
Figure 3: Unsuccessful casting due to inappropriate cell size and strut radius.

After conducting many trials, it was concluded that minimum cell size should be larger than 4mm, as well strut radius should be no less than 0.1mm. Based on these dimensional constrains, new stochastic lattices were modelled 3D printed and manufactured. The results are illustrated in the following figure:

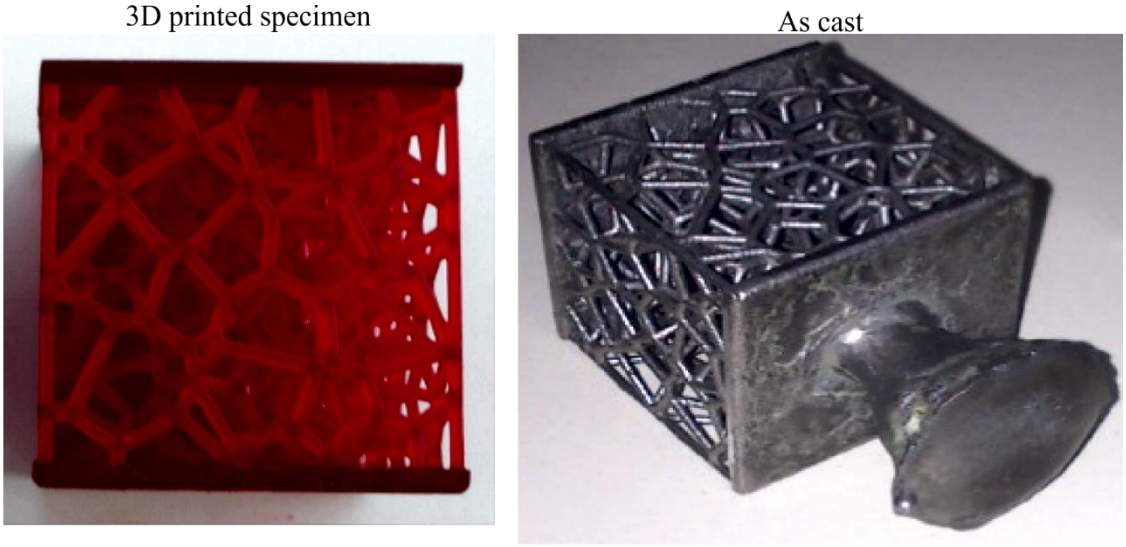

Resin: Asiga SuperCAST, Printing layer height: 10μm
Casting material: Steel 304
Figure 4: Successful casting after proper modification of geometrical constrains.

The number of manufactured specimens, the casting material, as well as geometric properties of modelled structures are provided in table 1.

Table 1. Manufactured specimens.

Casting material	Shape	Dimensions [mm]	# of specimens	Porosity [%]	Strut radius [mm]
Aluminium A1100	Cylinder	ØXH 31X31	3	76.7	0.7
Aluminium A1100	Cube	31X31X31	3	76.7	0.7
Stainless steel 304	Cube	31X31X31	1	87.4	0.5

As it is observed, usable specimens with fine geometric features were possible to manufacture with stainless steel 304. The melting temperature of aluminium A1100 was not high enough, thus it was possible to fill the mold up to a point for specimens that had a strut radius of 0.5mm. On the other hand, that was not observed for specimens with larger radius.

4. Mechanical tests

The compressive experiments were conducted using an INSTRON 8801 servohydraulic machine. Its maximum axial load capacity is ±100kN. Control of the 8801 is achieved with the use of a controller and a PC, equipped with appropriate software that provides complete control of the system. During the test, load or displacement control can be achieved, in order to meet the required target. The testing is procedure programmed accordingly with the use of an appropriate application for static tests, which accompanies the testing machine (Bluehill). All specimens were slightly prestressed (<10N) in order to eliminate any planarity errors. Thereafter, a constant compression displacement rate was applied to the specimen, equal to 2mm/min. The compression force was continuously monitored through the installed load cell. Similarly, the position of the load piston was registered. All tests were carried out until displacement was equal to 30% of the specimen's height.

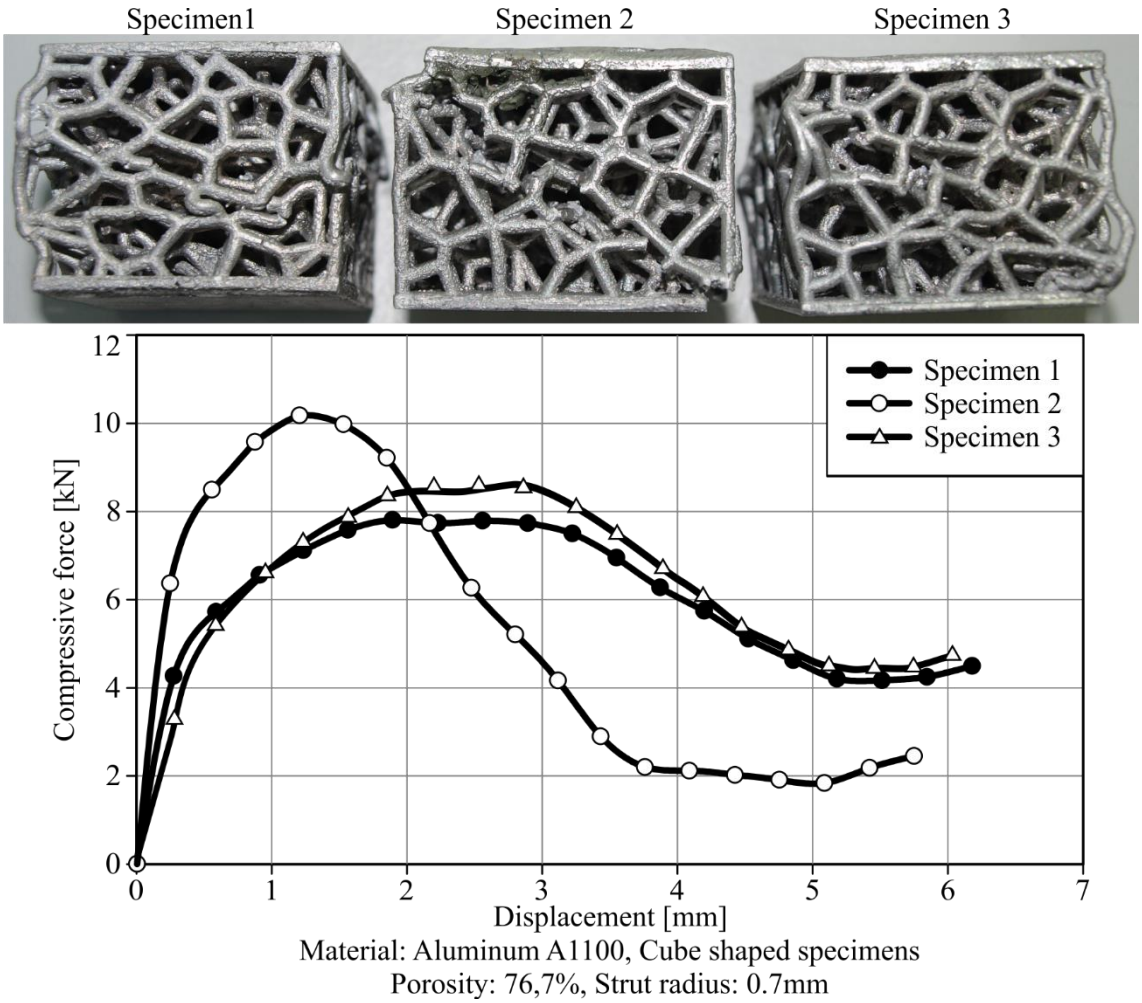

Figure 5: Experimental results for cube shaped aluminium stochastic lattice specimens.

The depicted mechanical behaviour, as it is presented in the form of compression force – displacement curves in figure 5, was unexpected. Two of the three specimens (one and three) exhibit similar behaviour, as their curves present small differences. Specimen #2 shows a different behaviour, indicating a deviation on the experimental parameters. The common observation between all specimens is the small (in specimens one and three) or completely absent (in specimen two) of the expected plateau region. The main characteristic of this region is the structure capability to retain a constant force value while deforming for a significant displacement range. Specimens one and three seem to develop such a region during compression for a displacement range approximately between 1.8 and 2.8mm, which is quite limited. Specimen two does not seem to develop this region. Rather than developing a plateau region, a premature collapse is engaged, which is also unexpected for a ductile material as aluminium, as it is also shown in the diagram of figure 5. Although metallographic analysis is necessary to investigate microstructural characteristics, the immediate quenching into water, which was applied to remove investment material, seems to be the cause of the limited material elongation. The same behavior was observed also for the cylindrical aluminum specimens. (45°)

On the other hand, the mechanical behavior of the stainless steel specimen, as it is presented in figure 6, did not demonstrate any surprises. The plateau region starts when the specimen's displacement reaches 2mm and extends beyond the illustrated displacement range, since there isn't an abrupt change in force value that would indicate a transition to the densification area. A minor change of the curve's tangent is observed when the compression displacement lies between 5 and 7mm. As it will be presented in the next section, contact between struts is initiated in the specific displacement region, causing the slight increment of the registered force value.

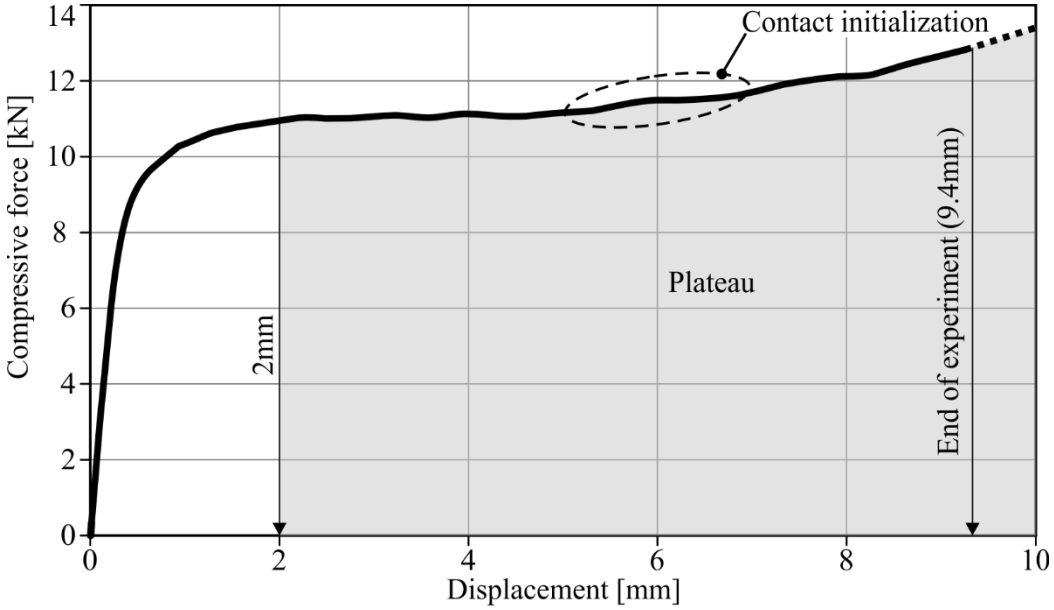

Material: Stainless Steel 304, Cube shaped specimens
Porosity: 87.1%, Strut radius: 0.5mm

Figure 6: Experimental results for cube shaped stainless steel stochastic lattice specimens.

5. FE assisted calculations

The finite element analysis of the compression response of the generated foam geometry was conducted using Deform 3D FEA software. The simulation of the compression of the modeled stochastic lattice structure involves large unconstrained plastic deformation under variable strain rates and localized phenomena due to the variable cross sectional geometry of the foam. The rigid-viscoplastic formulation, in which the elasticity effects are completely neglected, is applied to this analysis. This is a valid assumption since the plastic strains are typically orders of magnitude greater than the elastic ones. In order to represent the evolution of the deformed geometry, the updated Lagrangian description of motion is used, i.e. the mesh follows the deformation of the solid. However, one of the main limitations of Lagrangian formulations for large plastic deformation problems is the excessive distortion of the elements that is caused, leading to unacceptably small time steps and numerical instability of the solution. A viable way to overcome this difficulty is to simulate compression by continuously remeshing (or rezoning) the plastic workpiece (foam).When certain conditions are met, such as zero or negative element Jacobians in one or more elements, a remeshing of the deformed area that triggered the event is necessary and an automatic mesh generation method is used to facilitate the convergence. Also, an adaptive meshing is applied in order to resolve steep gradients that may be present in the solution. Weighting factors can be individually assigned for specifying the relative mesh density to regions of high curvature, steep strain or strain rate. In this way, mesh adaptability can maintain a high-quality mesh in severely deformed zones.

The stochastic lattice structure was modelled as an elasto-plastic object and meshed using 4-node tetrahedral elements. Due to the high total surface area of the modelled specimen and its complicated geometry, a total of nearly 900,000 elements were created in order to represent the imported volume with acceptable accuracy. A box-shaped simple rigid object in contact with the lattice was included in the finite element model setup to apply the compressive load by defining the displacement towards the specimen with constant but adjustable velocity, according to the strain rate desired. The opposite specimen side was simply supported by defining a z=0 displacement restriction. In order to assist solver convergence, the compressive speed was set equal to 0.5mm/s, which is higher than the one used during the experiments, but the resultant strain rate had a negligible effect on the compressive force. Also, an appropriate self-contact detection algorithm was used, to account for the added reaction force caused by structure's struts interaction. The generated structure was deformed up to approximately 50% of its size in the direction of compression.

The determination of the rate dependent material properties is of a great importance since high strain rates can differentiate the material mechanical response by a great extent. Several models have been proposed that try to approximate the viscoplastic behavior of materials over a wide range of strain rates and temperatures. The Johnson – Cook model, Zerilli – Armstrong and Norton – Hoff are characteristic examples of such models. Another method is the definition of the rate dependent material properties in table format. This method is simpler and can represent material behaviours not possible with the previously mentioned ones. The drawback is the table definition which is rather time consuming and difficult to edit. The developed FE model as well as the defined material properties for stainless steel 304 are presented in figure 7.

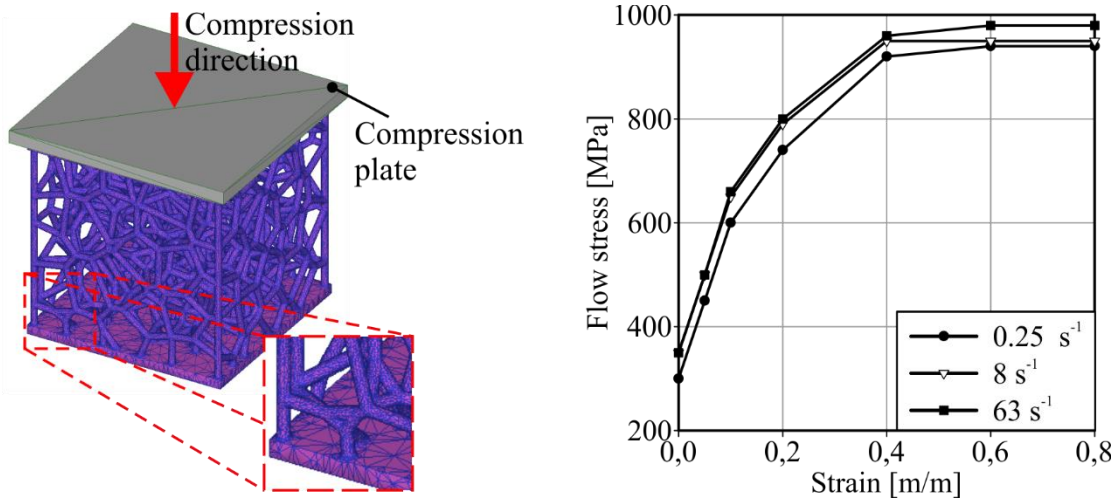

Figure 7: Developed FEA model and applied rate dependent material properties for stainless steel 304.

The simulation completed after solving 3100 steps, with a variable stroke (displacement) per step. A total of 13 remeshing steps were necessary to correct poorly formed elements during simulation. It took almost 7 days on an i7 3770K PC equipped with 32Gb of RAM. The saved data files had a size that reached 60Gb.

5.1. Simulation results

It was of high interest to check whether the calculated deformation could accurately capture the deformation of the specimen during experimental testing. As it is pictured in figure 8, the two geometries are almost identical.

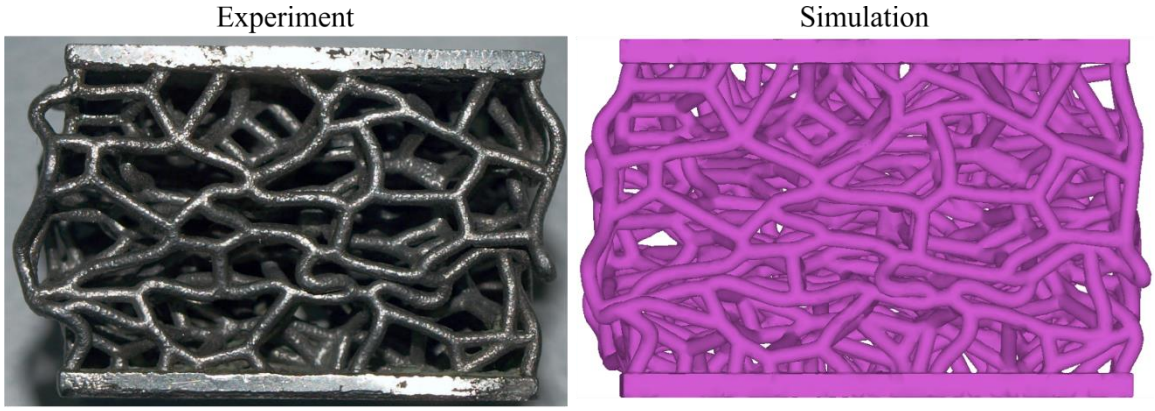

Material: Stainless Steel 304, Cube shaped specimens
Porosity: 87.1%, Strut radius: 0.5mm
Figure 8: Specimen deformation as depicted by experiment (right) and simulation (left).

The above mentioned result verifies that FEA, with proper model setup and material properties, is possible to deliver accurate results even in cases where geometry is very complex. On the other hand, the calculated compressive force presents a slight different behaviour. As it is presented in figure 9, up to 3.5mm both curves coincide. After this point, the calculated compressive force curve does not converge anymore with the measured one, although both of them exhibit an increasing trend. At the end of the experimental curve, the deviation between the two curves reaches 6.5%. This deviation can be attributed to a number of parameters such as:

- Defined material properties. The material data used for the FE model setup were provided with the FEA software. So it is not possible to describe the behaviour of the material used for castings, with an accuracy of 100%.
- Remeshing steps. During simulation it is necessary to rebuild the mesh at areas where element distortion exceeds quality criteria. After remeshing, an interpolation routine is applied to transfer the solution data from the old mesh to the new one. This process smooths the transferred solution data, as it can be observed at the various remeshing steps of figure 9, where the compressive force decreases abruptly, and it recovers after 50 to 60 solution steps.
- Elastoplastic material model. Force recovery is also caused by the elastoplastic material model. Due to remeshing, elastic deformation is lost, so in the next simulation steps the calculated deformation of the lattice structure lies within its elastic range. Thus, it is necessary to deform the lattice structure to regain its elastic portion, before any plastic deformation occurs. That procedure affects the compressive force calculation up to the point where material enters the plastic deformation region.

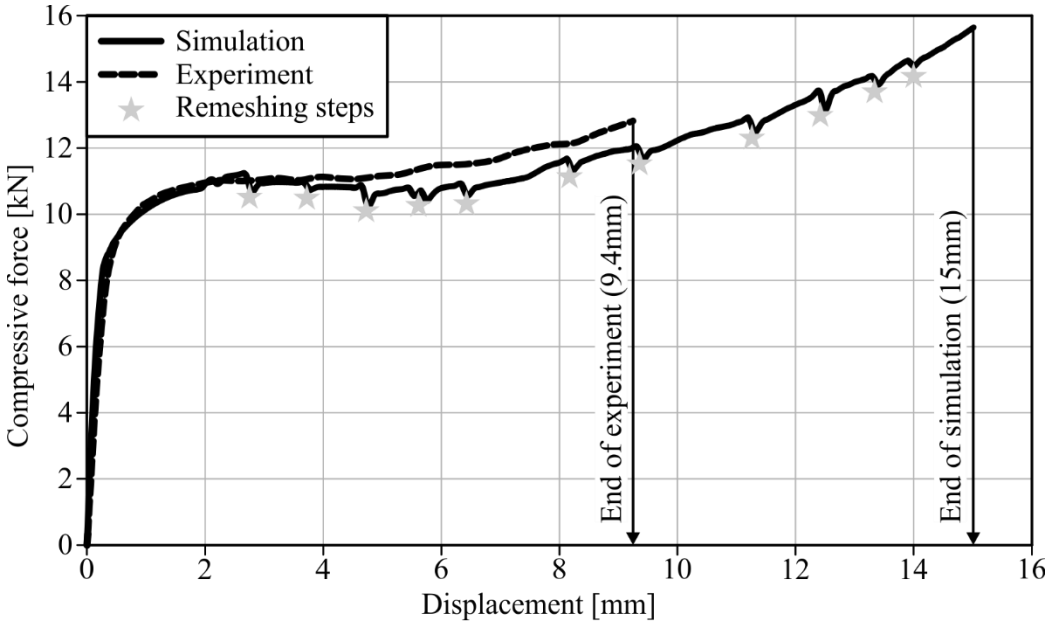

Material: Stainless Steel 304, Cube shaped specimens
Porosity: 87.1%, Strut radius: 0.5mm
Figure 9: Measured and FEA calculated compression force.

Another interesting simulation outcome is the progression of the number of contact sites. In figure 6 it was identified that contact is initiated between the displacement range of 5 to 7mm. As it was previously mentioned, a contact algorithm was defined during FE model setup. In figure 10, the contacted nodes as well as the contact area for 3 displacement values (5, 6, 7mm) are presented. As compressive displacement reaches 5mm, the first nodes begin to interact, but the effect on the compressive force value is negligible. At 6mm, the number of contact nodes is multiplied, also the total contact area becomes 1.77mm^2, and the interaction between the ligaments starts to compensate on

force calculation. At 7mm the same trend is observed, thus it is verified that contact is established in the specific displacement range.

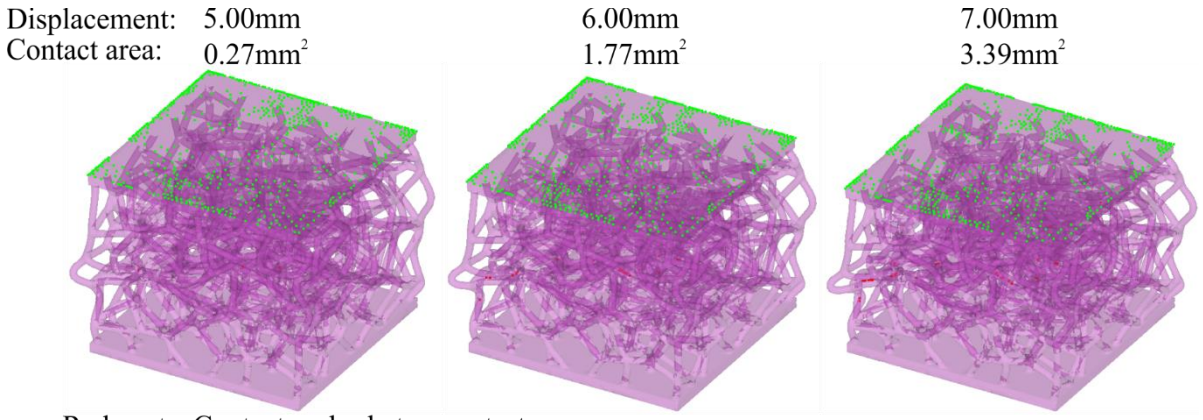

Red spots: Contact nodes between struts
Green spots: Contact nodes between specimen upper surface and compression plate

Figure 10: Evolution of contact area.

6. Conclusions

This work had an initial target to materialize stochastic lattice structures with a production method that permits the use of several materials. That was accomplished with the aid of 3D printing and investment casting. After several trials, the design and process parameters were optimized and successful castings were conducted. That success is a huge step towards manufacturing of random lattice structures with various materials, since the only alternative manufacturing method is 3D printing with metal powder (SLM or SLS), which imposes restrictions on material availability. Furthermore, the conduction of compressive material tests showed that the manufactured specimens exhibit very high load to weight ratio, a key parameter of metal foams. Also, the results of the FEA of the experimental procedure verified the FE model setup and proved that is possible to design stochastic structures based on FEA results before manufacturing.

7. References

[1]. Banhart J 2000 Manufacturing routes for metallic foams *JOM* **52** 22-27
[2]. Gibson L J and Ashby M F 1997 *Cellular Solids – Structure and Properties* (Cambridge: Cambridge University Press)
[3]. Li K, Gao X L and Subhash G 2006 Effects of cell shape and strut cross-sectional area variations on the elastic properties of three-dimensional open-cell foams *J. Mech. Phys. Solids* **54** 783–806
[4]. Alkhader M and Vural M 2008 *Mechanical response of cellular solids: Role of cellular topology and microstructural irregularity* Int. J. Eng. Sci. **46** 1035–1051
[5]. Raj S V 2011 Microstructural characterization of metal foams: An examination of the applicability of the theoretical models for modelling foams *Mat. Sci. Eng. A-Struct.* **528** 5289–5295
[6]. Jang W Y, Kyriakides S and Kraynik A M 2010 On the compressive strength of open-cell metal foams with Kelvin and random cell structures *Int. J. of Solids Struct.* **47** 2872–2883
[7]. Gong L and Kyriakides S 2005 Compressive response of open cell foams Part II: Initiation and evolution of crushing International *Int. J. of Solids Struct.* **42** 1381–1399
[8]. Jang W Y, Kraynik A M and Kyriakides S 2008 On the microstructure of open-cell foams and its effect on elastic properties *Int. J. of Solids Struct.* **45** 1845–1875
[9]. Borovinšek M and Ren Z 2008 Computational modelling of irregular open-cell foam behaviour under impact loading *Materialwiss. Werkst.* **39** 114–120.
[10]. Alsayednoor J, Harrison P and Guo Z 2013 Large strain compressive response of 2-D periodic representative volume element for random foam microstructures *Mech. Mater.* **66** 7–20.

[11]. Michailidis N 2011 Strain rate dependent compression response of Ni-foam investigated by experimental and FEM simulation methods *Mat. Sci. Eng. A-Struct.* **528** 4204–4208
[12]. Ahmadi S, Yavari S, Wauthle R, Pouran B, Schrooten J, Weinans H and Zadpoor A 2015 Additively Manufactured Open-Cell Porous Biomaterials Made from Six Different Space-Filling Unit Cells: The Mechanical and Morphological Properties *Materials* **8** 1871–1896
[13]. Kadkhodapour J, Montazerian H, Darabi A C, Anaraki A P, Ahmadi S M, Zadpoor A A and Schmauder S 2015 Failure mechanisms of additively manufactured porous biomaterials: Effects of porosity and type of unit cell *J Mech Behav Biomed Mater* **50** 180–191
[14]. Wauthle R, Vrancken B, Beynaerts B, Jorissen K, Schrooten J, Kruth J -P and Van Humbeeck J 2015 Effects of build orientation and heat treatment on the microstructure and mechanical properties of selective laser melted Ti6Al4V lattice structures *Addit. Manuf.* **5** 77–84
[15]. Gaitanaros S and Kyriakides S 2015 On the effect of relative density on the crushing and energy absorption of open-cell foams under impact *Int. J. Impact Eng.* **82** 3–13
[16]. Gaitanaros S, Kyriakides S and Kraynik A M 2012 On the crushing response of random open-cell foams. International *Int. J. of Solids Struct.* **49** 2733–2743
[17]. Sotomayor O E and Tippur H V 2014 Role of cell regularity and relative density on elastoplastic compression response of 3-D open-cell foam core sandwich structure generated using Voronoi diagrams *Acta Mater.* **78** 301–313